Prediction and analysis of process failures by ANN classification during wire-EDM of Inconel 718

Abhilash P. M.*, D. Chakradhar

Department of Mechanical Engineering, Indian Institute of Technology Palakkad, Kerala, India, 678557

*Corresponding author: abhilashpm184@gmail.com, ORCID ID: 0000-0001-5655-6196

Abstract

Wire breakages and spark absence are two typical machining failures that occur during wire electric discharge machining, if appropriate parameter settings are not maintained. Even after several attempts to optimize the process, machining failures cannot be eliminated completely. An offline classification model is presented herein to predict machining failures. The aim of the current study is to develop a multiclass classification model using an artificial neural network. The training dataset comprises 81 full factorial experiments with three levels of pulse-on time, pulse-off time, servo voltage, and wire feed as input parameters. The classes are labeled as normal machining, spark absence, and wire breakage. The model accuracy is tested by conducting 20 confirmation experiments, and the model is discovered to be 95% accurate in classifying the machining outcomes. The effect of process parameters on the process failures is discussed and analyzed. A microstructural analysis of the machined surface and worn wire surface is conducted. The developed model proved to be an easy and fast solution for verifying and eliminating process failures.

Keywords *Wire-EDM; process failure; spark absence; wire breakage; ANN classification; failure prediction.*

Article Highlights

- The aim of this study is to develop a multiclass ANN classification model that predicts process failures during wire-EDM of Inconel 718.
- Prediction of process failures is industrially significant because it can reduce process interruptions, thereby improving the sustainability of wire-EDM. The developed model is 90% accurate in classifying process failures such as wire breakage and spark absence.
- The analysis of failure mechanisms and the effects of process parameters on different machining outcomes are discussed.

Declarations

- **Funding**: No funding was received.
- **Conflicts of interest**: The authors declare that they have no known competing financial interests or personal relationships that could have appeared to influence the work reported herein.
- **Availability of data and material** – Not applicable
- **Code availability**- Not applicable

This is a peer-reviewed, accepted author manuscript of the following article: P. M, A., & Chakradhar, D. (2020). Prediction and analysis of process failures by ANN classification during wire-EDM of Inconel 718. Advances in Manufacturing, 8(4), 519-536. https://doi.org/10.1007/s40436-020-00327-w

1. Introduction

Wire electric discharge machining (wire-EDM) is a nontraditional machining process that can cut any electrically conductive material, irrespective of its hardness. The process is applicable for machining components that are difficult to machine using conventional techniques. The process offers many advantages over traditional machining processes, such as lower cutting forces and minimal residual stresses. Even though wire-EDM is extremely accurate and economical, the prediction of responses is challenging because many uncontrollable factors are involved [1]. Parametric optimizations have been performed to achieve maximum results from wire-EDM. However, process failures occurred even after parameters were tuned owing to the inherent variability in wire-EDM. Two typical process failures associated with wire-EDM are wire breakage and spark absence.

Material removal occurs by controlled repetitive sparks. The supplied pulsed direct current voltage comprises “pulse on” and “pulse off” durations. During the pulse-on time, the dielectric fluid between the conductive workpiece and wire electrode ionizes and high-energy discharge spark occurs. During the pulse-off time, debris is flushed off and the dielectric property is restored in the spark gap. The inter-electrode gap (spark gap) is controlled by the servo voltage. Because material removal occurs from the wire electrode, fresh wire is continuously fed to the machining zone from the wire spool [2].

Several researchers have analyzed the reasons for wire-EDM process interruptions. Saha et al. [3] developed a finite element model to predict heat distribution in a wire, based on which parametric optimization was performed to prevent wire breakages. Fedorov et al. [4] analyzed the implicit and explicit causes of wire breakage failures; they discovered that implicit and explicit failures were caused by debris accumulation and short circuits, respectively. Meanwhile, machine feedback violation was discovered as the primary cause of the failures. Gamage and Desilva [5] studied the effect of machining interruptions on energy utilization. They discovered that 23% additional energy was utilized during wire breakages and rethreading. Okada et al. [6] performed CFD analysis to investigate the effects of flushing pressure on wire vibration and wire breakage. They discovered that debris accumulation and wire deflections were main causes of wire breakage.

Additionally, machining failures have been investigated from the perspective of sustainability and cost optimization. Yeo et al. [7] developed a cost–tolerance relationship model for wire-EDM during the machining of medium carbon steel plates. D’Urso et al. [8] developed a model to predict the manufacturing costs associated with micro-EDM drilling

considering both fixed and variable costs. The experiments were conducted on steel and WC materials. Furthermore, D'Urso et al. [9] conducted a separate study on the micro-EDM drilling of WC plates for cost minimization. Subsequently, the CCD design of RSMs was performed to derive regression equations for the responses. These studies investigate the effects of variable costs on the overall efficiency of the process. By classifying and modeling machining failures in wire-EDM, the proposed model can substantially reduce the process interruptions and electrode consumption, thereby improving the process sustainability and cost efficiency.

The artificial neural network (ANN) is regarded as a capable soft computing tool to model stochastic processes. The model can handle higher-dimensional data and nonlinearities better than other conventional and soft computing techniques. Therefore, several researchers have attempted to model manufacturing process responses using ANNs [10-14].

Machining failure detection models have been developed previously, and most of them involve online monitoring and wire breakage prevention [15 -17]. Wang and Rajurkar [18] developed an algorithm to predict wire ruptures by monitoring sparking frequencies. Luo [19] investigated the wire breakage mechanism with an emphasis on the wire strength. Subsequently, Kwon and Yang [20] observed that owing to instability in the spark gap, wire ruptures can occur even at constant sparking frequencies. They studied the advantages of considering instantaneous discharge energy over sparking frequencies for wire rupture prediction and prevention. Cabanes et al. [21] proposed an early detection method for forecasting wire breakages. They built a database of various failure situations, based on which predictions were made. A real-time signal acquisition system was set up for the predictive model. The developed algorithm alerts the user of potential wire breakage situations based on discharge energy, current, and ignition delay. However, the model functions only online and does not address instabilities due to excess open-circuit pulses. Liao and Woo [22] designed a fuzzy-logic-based condition monitoring algorithm to avoid process failures in WEDM. The system has an online pulse classifier that computes the short-circuit ratio in real time. The feed and pulse-off time are regulated based on monitored data. Bufardi et al. [23] developed an offline–online fuzzy logic model for wire-EDM monitoring to predict future defects. The offline fuzzy logic model predicts process responses, whereas the online model adjusts the input parameters in real time to avoid machining defects. However, these fuzzy-based systems are expert-knowledge dependent and not trainable. Fuzzy systems are based on a rule set and cannot be trained by adjusting the model parameters (weights and biases). Failure situations in wire-EDM are often more complicated than those defined by a set of rules, and modeling failures by fuzzy rules can be inaccurate. Kumar and Choudhury [24] attempted to model

failures by performing experiments based on the central composite design of a response surface methodology. They developed a regression model to predict the frequency of process interruptions. Even though the model functions offline, the CCD design is an extremely simplified experimental design that may overlook factor interactions that are critical for the model accuracy. In addition, unlike an ANN model, developing a regression model requires prior assumptions regarding the type of function (order of the polynomial, or exponential) between the parameters and response [25].

The online monitoring models discussed thus far require a separate multisensorial setup for real-time data acquisition and analysis. Such systems are costly and require high computational power to analyze and monitor the machine health situation. Most of the developed online monitoring systems detect a forthcoming failure during machining but cannot perform any real-time preventive action. This renders the process unsustainable even with the monitoring system. In such situations, an offline model with sufficient training data is often more relevant to prevent failure events. The key advantage of an offline model is that it informs the user regarding potential machining failures before machining is commenced, unlike online monitoring. Hence, the proposed classification model renders the process more sustainable and energy efficient. Even in cases where online monitoring is required, the proposed model can still be useful in setting the initial process parameters, thereby reducing the possibilities of real-time failure situations significantly. The difficulty in developing such a classification model is due to complex phenomena associated with different failure modes. The process is extremely stochastic, with several parameter interactions. In addition, an extensive experimental database is required to set up such a system. The former issue can be overcome using a trained ANN classification model, which can model extremely complicated processes. Eighty-one full-factorial training experiments and 20 additional confirmation experiments were conducted to encompass the entire input parameter working range of the wire-EDM machine. This ensured that both the failure modes associated with all the possible parameter combinations were considered.

A review of the literature study revealed that several studies have been conducted to predict and optimize the process outcomes of Wire-EDM. However, an effective offline machining failure classification model that considers multiple failure modes for electric discharge machining is yet to be developed. The proposed ANN classifier can forecast machining failures for any input parameter set. The objectives of the current experimental study are as follows:

(a) Classify the process outcomes into failure and non-failure conditions. The two failure classes are spark absence and wire breakage, whereas the non-failure class is normal machining.
(b) Analyze the mechanism of failure conditions and analyze the effects of process parameters on process failures.

2. WEDM Process Failures

In wire-EDM, any of the following three outcomes are expected: spark absence, wire breakage, and normal machining. Among these, the first two are considered process failures. These failures occur because of non-ideal conditions in the spark gap between the wire electrode and workpiece. In this study, only process interruptions were considered as machining process failures. Process interruptions are those that cause the machining process to discontinue/delay, resulting in energy and material wastage. Process interruptions such as wire breakages and spark absence render the process unsustainable and cost inefficient [5, 19].

2.1 Failure modes

2.1.1 *Wire breakages*

The conductivity of the dielectric in the spark gap changes continuously owing to the interaction with previously removed microparticles known as debris. The higher the presence of the debris, the higher is the electrical conductivity. This causes sparks of higher intensity (known as arc or short-circuit sparks) and hence wire breakage. This undesired situation is extremely difficult to control because the exact amount of debris present in the spark gap at any time is unpredictable. Typically, debris accumulation occurs when the pulse-off time or spark gap distance is inadequate. If the wire feed is extremely low, then multiple craters can occur in the same area on the wire surface, which can result in wire breakages. This type of failure is more frequently expected if the parameters are set to achieve the maximum cutting speed [21].

It can be inferred from the process mechanism that the pulse-on time, servo voltage, and pulse-off time significantly effects machining failures due to wire breakage. If the pulse-on time is longer, then the discharge energy is higher; hence, the amount of material removed from both the workpiece and wire electrode is higher. If the amount of debris is larger than the flushing capacity, then excess debris will start to accumulate in the spark gap. Short-circuit and arc discharges due to debris accumulation and spark gap bridging eventually result in wire

breakages. If the servo voltage is lower, then the spark gap is narrower; consequently, gap bridging is more likely to occur. In addition, if the pulse-off time is shorter, then the time available to flush off the debris from the spark gap is shorter and gap bridging may occur. The situation worsens if the wire feed rate is low because the possibility of repeated sparks occurring at the same wire spot is greater. In this case, the wire strength is weakened by excessive wire surface damage and wire failure will occur.

Any one or the combinations of the parametric conditions above are potential causes of machining failures due to wire breakage. Even though it is safe to assume that the combination of high pulse-on time, low servo voltage, and low pulse-off time will cause process failure, similar intuitive predictions are extremely difficult for the other parameter combinations. Therefore, without a classification model, the prediction of process failures is extremely difficult because of the complicated nature of interactions between process parameters.

2.1.2 Spark absence

Another type of failure can occur when the spark gap is not ideal for sustaining repeated sparks. The open-circuit voltage supplied across the electrodes should be sufficiently high to break the dielectric barrier. If such an unideal situation arises when the discharge energy cannot surpass the dielectric barrier, then the discharge will not occur for the entire voltage pulse duration [25]. Such pulses are known as open-circuit pulses (where the discharge current is absent). If the proportion of open pulses predominates the pulse train, then machining will not occur because of spark absence. This type of failure is more frequently expected when the parameters are set to maximize the surface quality.

Spark absence occurs when the open-circuit pulses predominate the pulse cycle. In such situations, normal spark discharges are either absent or inadequate for machining. One of the primary reasons for spark absence is the large spark gap. In this case, the energy is insufficient to overcome the dielectric barrier, thereby preventing any discharge between the wire electrode and conductive workpiece. Hence, if the servo voltage, which determines the spark gap, is set at an extremely high value, the spark gap will be correspondingly large. Such parameter combinations are at risk of process failure because of spark absence [26].

The other parameters that affect spark absence are the pulse-on and pulse-off times. If the pulse-on time is extremely low, then the spark discharge energy may be insufficient to cause material removal via melting and vaporization. In addition, if the pulse-off time is extremely high, then the spark frequency will be extremely low, which may result in either no machining or machining with an extremely low material removal rate.

2.2 Normal machining

In normal machining, increasing the pulse-on time improves the productivity and reduces the surface finish. This is because a higher pulse-on time implies a higher amount of material removed per spark, causing larger craters on the machined surface. The higher the servo voltage, the lower is the productivity, but the better is the surface finish. A higher servo voltage increases the spark gap and improves the flushability. In addition, if the pulse-off time is higher, the productivity decreases but the surface finish will be better. A higher pulse-off time implies more time to flush away the debris. However, it also means a lower spark frequency, resulting in a decreased cutting rate. A higher wire feed rate improves the flushability and produces better surfaces compared with a lower wire feed rate.

The classifications of machining outcomes are detailed in Table 1.

Table 1 Classification of machining outcomes

Machining outcomes	**Reason**	**Effect on machining**
Spark Absence	High spark gap, less discharge energy	Machining does not happen, zero cutting speed
Normal spark machining	Ideal conditions for machining	Machining happens typically
Wire breakage	Narrow spark gap, high discharge energy, less pulse off time	Process discontinuity, Machined surface defects, require manual or auto rethreading

2.3 Classification problem

Classification is a supervised learning technique in machine learning. The classification problem involves identifying the class of a particular sample from the training data, which contain a set of samples (data points) and their corresponding classes. Here, the class is the group or category to which each data point belongs. Each class is labeled suitably. The three class labels in this case are “wire breakage,” “normal spark machining,” and “spark absence.” The common features of all the samples belonging to a particular class are learned from the training dataset. This information is used to identify the class of any new sample, which is not part of the original training set. One method of classification is using ANNs.

Generally, classification models attempt to determine a decision boundary that separates the classes under consideration. The decision boundary of complex events involving inter-relationships between multiple factors will be highly nonlinear and multidimensional. As the

complexity of the boundary increases, decision making becomes more difficult. In this case, the data points are spread out in a four-dimensional space. The ANN classification model is considered the most efficient tool for addressing high-dimensional problems, where highly nonlinear methods are essential to process the available information. The model can detect factor interactions that may be unidentifiable via conventional classification techniques. Moreover, the ANN model can be tuned to prevent overfitting and underfitting [24].

An ANN uses several interconnected neurons to perform classification. The neurons are presented as input, hidden, and output layers. The connection between any two neurons will have a weight associated to it. Each neuron performs a weighted sum and often applies a function to it. This output is transferred to the next layer, and so on. The weights on the connections are tuned during the training phase by reducing the difference between the predicted and actual responses. The neural network attempts to identify the decision boundary (a hyperplane) in a four-dimensional space (with four input parameters as the axes) to separate three classes. Once trained, the neural network model can perform classification. The classification model calculates the probability (likelihood) of a parameter combination belonging to a particular output class (label). For any input parameter combination, the model calculates the probability of occurrence of all three events (spark absence, wire breakage, and normal machining). The class with the highest probability of occurrence is the predicted class [27].

Because the classification model classifies the data points into multiple classes, the problem is known as multiclass neural network classification. Fig. 1 shows the structure of a multiclass neural network classification model.

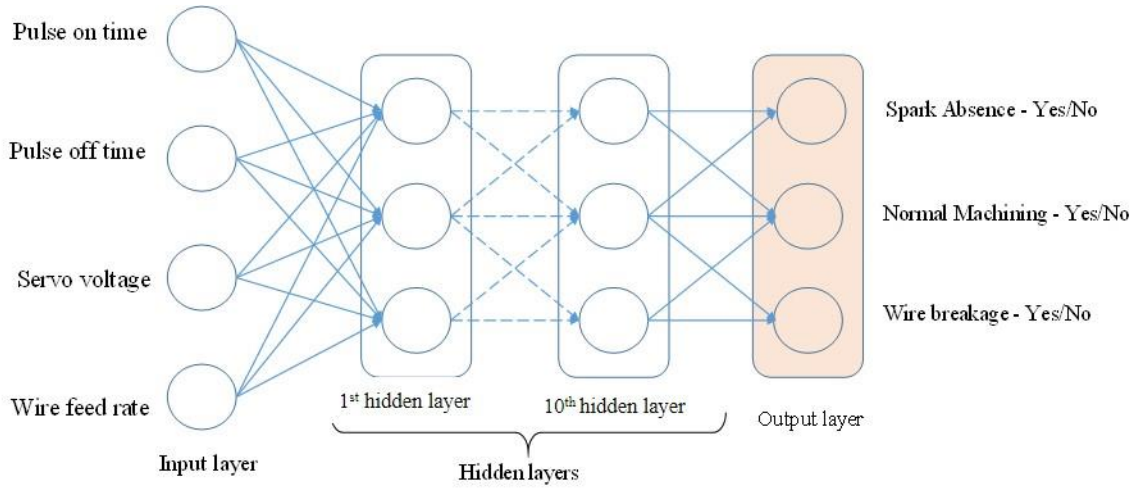

Fig. 1 Structure of multi-class neural network classification model

3 Materials and Methods

3.3 Materials

Inconel 718 was selected as the workpiece material because of its industrial applications in high-temperature applications. This material is known for its excellent mechanical strength, fatigue, and creep resistance at elevated temperatures [28]. The mechanical and chemical properties of Inconel 718 are listed in Tables 2 and 3. The wire electrode material selected for the study was a hard zinc-coated brass of diameter 0.25 mm. Coated electrodes were selected because their overall efficiency is better compared with that of uncoated electrodes [29].

Table 2 Properties of Inconel 718

Property	Value
Density	8.19 g/cm^3
Melting Point	1260 – 1336 ºC
Specific Heat	435 J/kg K
Average Coefficient of thermal expansion	13 μm/m K
Thermal Conductivity	11.4 W/m K
Ultimate Tensile strength	1240 MPa

Table 3 Chemical composition of Inconel 718

Element	Ni	Fe	Cr	Nb	Mn	C	Co	Al	Si	Ti	Mo	Others
Weight (%)	51.05	19.43	18.70	5.7	0.07	0.04	0.2	0.56	0.08	1.01	3.1	0.06

3.4 Experimental plan

An ‘Electronica’ Eco-cut wire-EDM machine was used in this study, as shown in Fig. 2. Straight cuts of 10 mm were cut in each run. Each experimental run was repeated thrice to eliminate experimental errors. The input parameters considered for the analysis were the pulse-on time, pulse-off time, servo voltage, and wire feed rate. Each parameter was varied in three levels, as detailed in Table 4. The parameter ranges were selected based on the wire-EDM limits. Deionized water was used in this study. The dielectric flushing pressure and wire tension were maintained constant. Because four factors and three levels were involved, 81 full-factorial experiments were conducted, and the responses were analyzed. A full-factorial experimental design was selected instead of a fractional-factorial or Taguchi orthogonal array design because the profile machined was simple straight cuts, and the performance of the ANN model was better when the training dataset contained more data points.

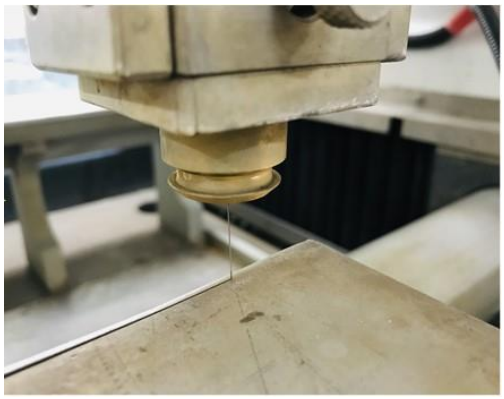

Fig. 2 Straight cuts machined by wire-EDM process

The responses considered for the analysis were the occurrence of wire breakage, spark absence, and normal machining. In the classification problem, the outcome (response variable) was in a categorical form, i.e., only binomial (0/1) values. In this study, "1" and "0" represent the occurrence and absence of the event, respectively. The events considered were "wire breakage," "normal spark machining," and "spark absence." The event "wire breakage" will have an outcome of "1" for a set of input parameters if the wire breaks before the 10 mm straight cut is finished with that setting. For that setting, the outcome for both "normal machining" and "spark absence" is "0." In addition, any set of input parameters can only result in one of those three events.

Table 4 Process parameters and levels

Parameters	**Pulse on time** T_{on} (µs)	**Pulse off time** T_{off} (µs)	**Servo voltage** SV (V)	**Wire feed rate** WF (m/min)
Level 1	100	20	20	3
Level 2	110	40	40	6
Level 3	120	60	60	9

In this study, Matlab R2019a was used to perform classification using an ANN. This technique involves learning the common features from trials of known categories to classify samples of unknown categories. The model developed was verified by conducting confirmation experiments.

4 Results and discussion

A feedforward back propagation neural network was used to classify the process outcomes. The neural network was trained based on 81 experimental trials and each of its corresponding

classes. The details are shown in Table 5. The neural network structure contained 10 hidden layers, with four nodes for the input layer and three nodes for the output layer. The optimum structure (4-10-3) was selected based on the overall model accuracy. The neural pattern recognition tool in MATLAB was used to design and develop the classification model. The number of hidden layers was varied from 1 to 15, and the most accurate structure was selected for the model. The MATLAB default number of neurons in each hidden layer was 10, which was not varied. The ANN structure is shown in Fig. 3. The ratios for training, testing, and validation were selected as 70%, 15%, and 15%, respectively. Therefore, 57 data points were available for training the model, whereas 12 data points were available for testing and validation. The Softmax function was used to classify the machining outcomes. The classification model provided the probability distribution of the input vectors in different classes. In the multiclass classification, the summation of the responses should add up to 1 because the classes were mutually exclusive.

Table 5 Experimental results

S. No.	Input Parameters				Observed Outcomes		
	T_{on} (µs)	T_{off} (µs)	Servo voltage (V)	Wire feed (m/min)	Spark Absence	Wire Breakage	Normal Machining
					"1" – Occurrence of an event "0" – Absence of an event		
1	100	20	20	3	0	0	1
2	100	20	20	6	0	0	1
3	100	20	20	9	0	0	1
4	100	20	40	3	0	0	1
5	100	20	40	6	0	0	1
6	100	20	40	9	0	0	1
7	100	20	60	3	1	0	0
8	100	20	60	6	0	0	1
9	100	20	60	9	0	0	1
10	100	40	20	3	0	0	1
11	100	40	20	6	0	0	1
12	100	40	20	9	0	0	1
13	100	40	40	3	0	0	1
14	100	40	40	6	0	0	1
15	100	40	40	9	0	0	1
16	100	40	60	3	1	0	0
17	100	40	60	6	1	0	0
18	100	40	60	9	1	0	0
19	100	60	20	3	1	0	0
20	100	60	20	6	1	0	0
21	100	60	20	9	0	0	1
22	100	60	40	3	1	0	0
23	100	60	40	6	1	0	0
24	100	60	40	9	1	0	0
25	100	60	60	3	1	0	0

26	100	60	60	6	1	0	0
27	100	60	60	9	1	0	0
28	110	20	20	3	0	1	0
29	110	20	20	6	0	1	0
30	110	20	20	9	0	1	0
31	110	20	40	3	0	0	1
32	110	20	40	6	0	0	1
33	110	20	40	9	0	0	1
34	110	20	60	3	0	0	1
35	110	20	60	6	0	0	1
36	110	20	60	9	0	0	1
37	110	40	20	3	0	1	0
38	110	40	20	6	0	1	0
39	110	40	20	9	0	1	0
40	110	40	40	3	0	1	0
41	110	40	40	6	0	0	1
42	110	40	40	9	0	0	1
43	110	40	60	3	0	0	1
44	110	40	60	6	0	0	1
45	110	40	60	9	0	0	1
46	110	60	20	3	0	0	1
47	110	60	20	6	0	0	1
48	110	60	20	9	0	0	1
49	110	60	40	3	0	0	1
50	110	60	40	6	0	0	1
51	110	60	40	9	0	0	1
52	110	60	60	3	0	0	1
53	110	60	60	6	0	0	1
54	110	60	60	9	0	0	1
55	120	20	20	3	0	1	0
56	120	20	20	6	0	1	0
57	120	20	20	9	0	1	0
58	120	20	40	3	0	1	0
59	120	20	40	6	0	1	0
60	120	20	40	9	0	1	0
61	120	20	60	3	0	1	0
62	120	20	60	6	0	0	1
63	120	20	60	9	0	0	1
64	120	40	20	3	0	1	0
65	120	40	20	6	0	1	0
66	120	40	20	9	0	1	0
67	120	40	40	3	0	1	0
68	120	40	40	6	0	1	0
69	120	40	40	9	0	1	0
70	120	40	60	3	0	0	1
71	120	40	60	6	0	0	1
72	120	40	60	9	0	0	1
73	120	60	20	3	0	0	1
74	120	60	20	6	0	0	1
75	120	60	20	9	0	0	1
76	120	60	40	3	0	0	1
77	120	60	40	6	0	0	1
78	120	60	40	9	0	0	1
79	120	60	60	3	0	0	1
80	120	60	60	6	0	0	1
81	120	60	60	9	0	0	1

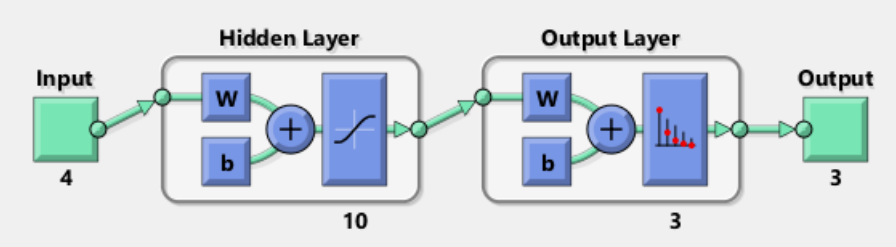

Fig. 3 ANN structure for the failure class prediction

3.1 Performance of classification model

Training was conducted using a scaled conjugate gradient backpropagation algorithm. Cross-entropy was the loss function selected to evaluate the performance of the classification model. The training was terminated when the cross-entropy error failed to decrease successively in six rounds of validations. The performance of the classification model on the test data is presented in a confusion matrix. The matrix identifies how accurately the data points are classified without mislabeling; this is termed as “confusion.” This matrix summarizes the classification results and provides the classification accuracy. The confusion matrix is shown in Fig. 4. The testing-phase accuracy of the model was 91.7%, and the overall accuracy was 90.1%.

Fig. 4 Confusion matrix for classification model

3.2 Confirmation Experiments

Confirmation experiments were conducted to verify the performance of the classification model. Twenty data points were selected randomly and used as inputs to the model. Experiments were conducted using these 20 input parameter settings, and the responses were recorded. The predicted class was compared against the experimental outcomes. It was discovered that 19 out of 20 machining responses were true to the predicted class, yielding a 95% accuracy in real-world situations. The results of these confirmation experiments are shown in Table 6. The class-wise performance evaluation of the classification model is shown in Table 7. The wire breakage probability for experiment number 3 was 0.52, and the normal machining probability was 0.48. The model predicted wire breakage because of the marginally higher breakage probability. However, because the probability difference between the two events was extremely low, the actual situation was in fact normal machining.

Table 6. Results of confirmation experiments

S. No.	Input Parameters				Outcomes	
	T_{on} (µs)	T_{off} (µs)	Servo voltage (V)	Wire feed (m/min)	Predicted Class	Actual Class
1	111	47	47	7	NM	NM
2	109	37	31	4	NM	NM
3	106	24	22	4	WB	NM
4	114	22	28	8	WB	WB
5	107	29	23	6	WB	WB
6	110	22	26	5	WB	WB
7	106	29	47	5	NM	NM
8	103	54	49	7	SA	SA
9	105	53	60	6	SA	SA
10	102	54	21	6	NM	NM
11	102	51	40	6	NM	NM
12	109	47	21	9	NM	NM
13	112	41	37	3	NM	NM
14	102	49	44	5	SA	SA
15	117	43	42	4	NM	NM
16	109	20	27	4	WB	WB
17	100	47	20	4	NM	NM
18	101	49	57	3	SA	SA
19	113	55	44	4	NM	NM
20	104	46	59	5	SA	SA

SA – Spark absence
WB – Wire breakage
NM – Normal machining

Table 7. Model performance during confirmation experiments

Performance	Classification result
Classification of normal machining	10/10
Classification of spark absence	5/5
Classification of wire breakages	4/5
Classification %	95 %

For further analysis, a MATLAB program was coded to generate all possible input vector combinations within the considered range. In total, 247,107 of such data points were classified using the model. An input parameter setting with less than 0.5 "normal machining" classification probability results in process failures either by wire breakage or spark absence.

Fig. 6 shows the three-dimensional (3D) scatter plot of the "normal machining class probability" vs. "pulse-on time" and "pulse-off time." For ease of representation, only two input parameters were considered for this plot. The maximum classification probability into the "normal machining" class is indicated in the green zone. The yellow zone has a probability of 0.4–0.6, whereas the red zone has a lower probability. The classification results of the confirmation experiments are shown with labels. Most of the normal machining classifications were from the green zone, and a few were from the yellow zone.

Similarly, Figs. 6 and 7 show the 3D scatter plot of the classification probability of the data points into "wire breakage" and "spark absence" classes. As expected, all the wire breakage and spark absence cases in the confirmation experiments belonged to the expected zones.

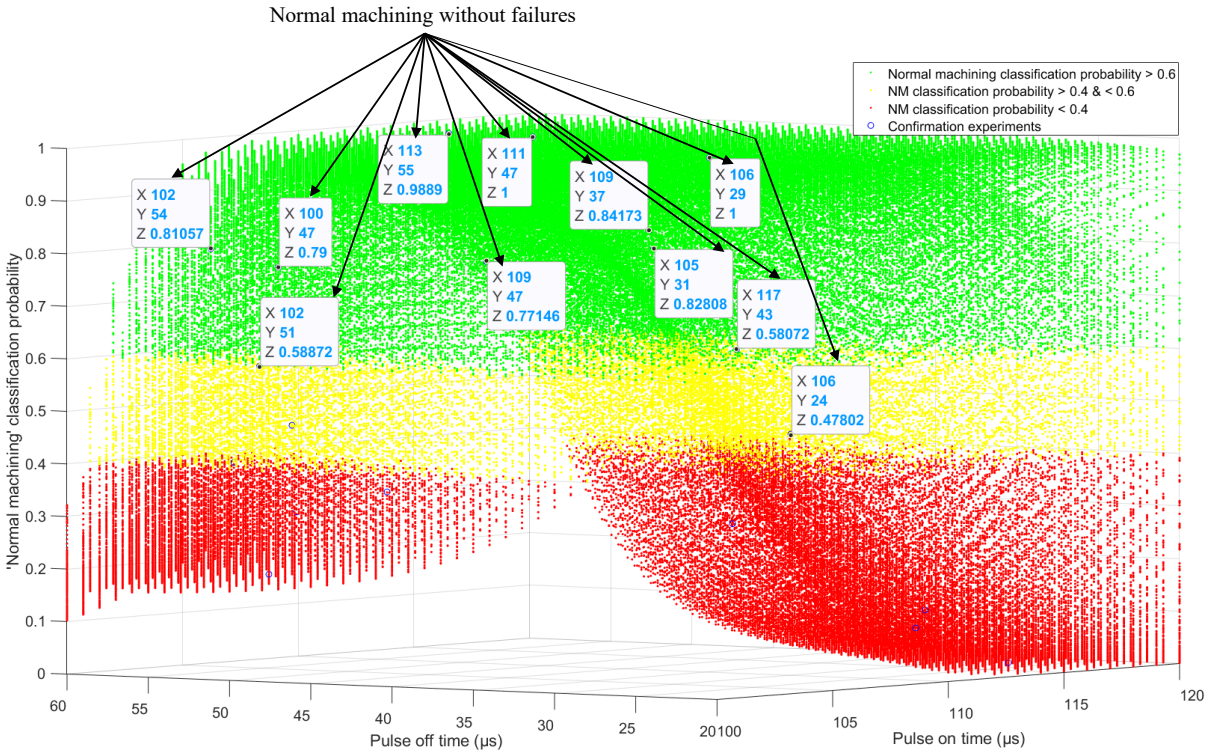

Fig. 5 Scatter plot of normal machining classification probability vs input parameters

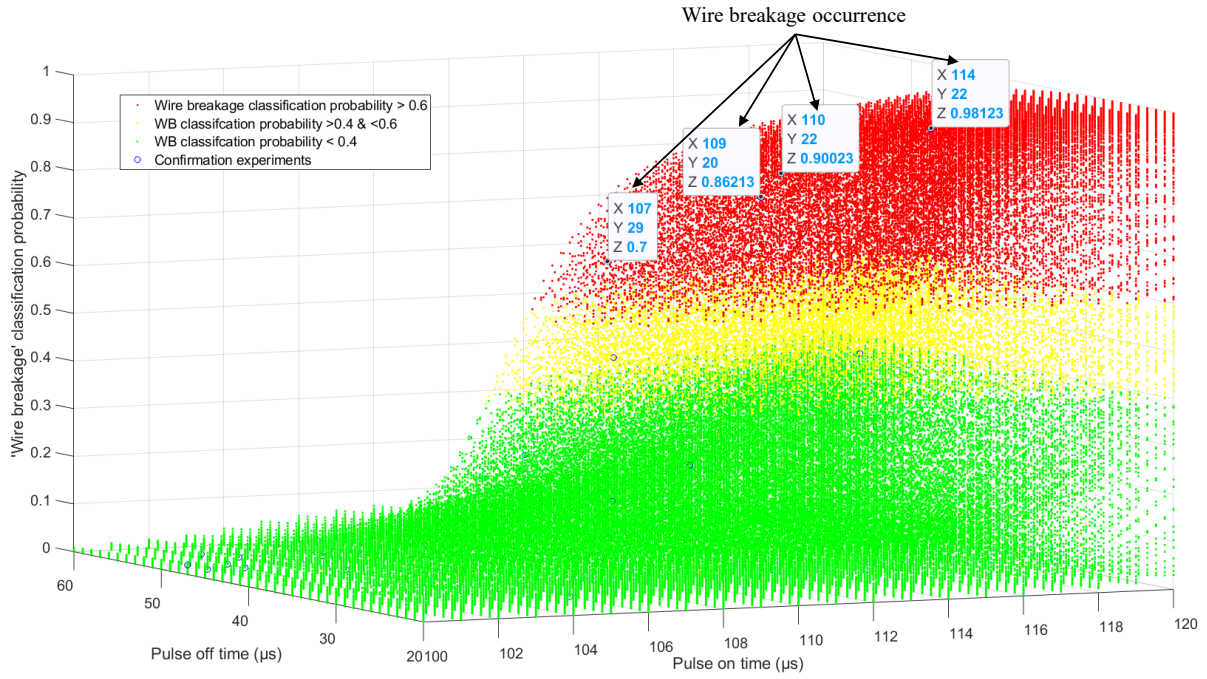

Fig. 6 Scatter plot of wire breakage classification probability vs input parameters

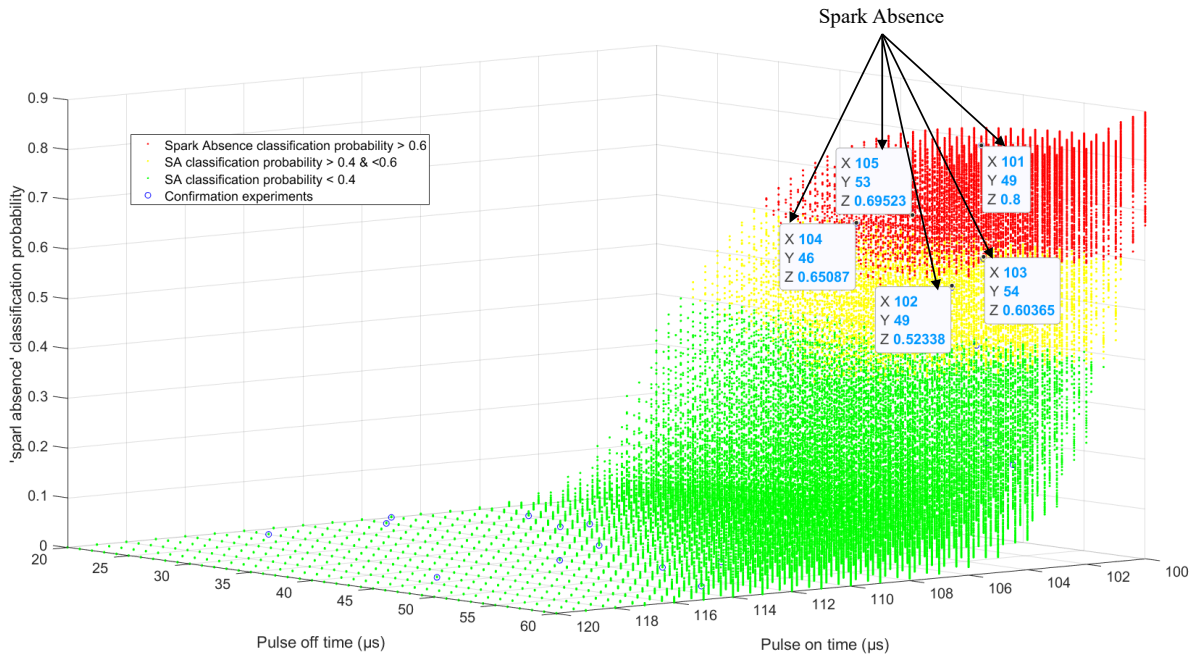

Fig. 7 Scatter plot of spark absence classification probability vs input parameters

3.3 Effects of machining parameters on process failures

The section analyses the mechanism of failure and the effects of the process parameters on the machined surface integrity.

3.3.1 Wire breakage analysis

The wire breakage mechanism was analyzed using scanning electron microscope images. The coated wire electrodes demonstrated better performances compared with the uncoated wire electrodes. Therefore, zinc-coated brass electrodes were used for the current study. The coatings protect the inner core from thermal shocks during the sparking mechanism by the "heat-sink effect." However, if the localized instantaneous process heat is extremely high, the coatings will be eroded quickly, exposing the inner copper core.

As discussed in Section 3, the classification model provides the probability distribution of an input vector into various response classes. To analyze the various stages of wire breakage, different wire surfaces in the increasing order of breakage probability were considered. Experiments 10, 13, 15, and 6 were selected with wire breakage probabilities of 0.01, 0.21, 0.42, and 0.9, respectively. Experiment number 6, with the maximum probability of wire breakage failure, resulted in wire breakage. Fig. 8 shows the microstructural comparison of the worn wire surfaces after these experimental runs. Fig. 8 (a) corresponds to experiment number 10 and shows minimal wire wear. The zinc coating is still visible in the image. Fig. 8 (b)

corresponds to experiment number 13, where the wire coatings were removed moderately, and the core brass wire was further exposed. Fig. 8 (c) corresponds to experiment number 15, which indicated significant wire wear with an extremely uneven surface morphology. The coatings were not distinguishable at this phase. Additionally, molten and resolidified debris are adhered to the wire surface. This indicates the occurrence of short-circuit sparks and spark gap bridging at this stage.

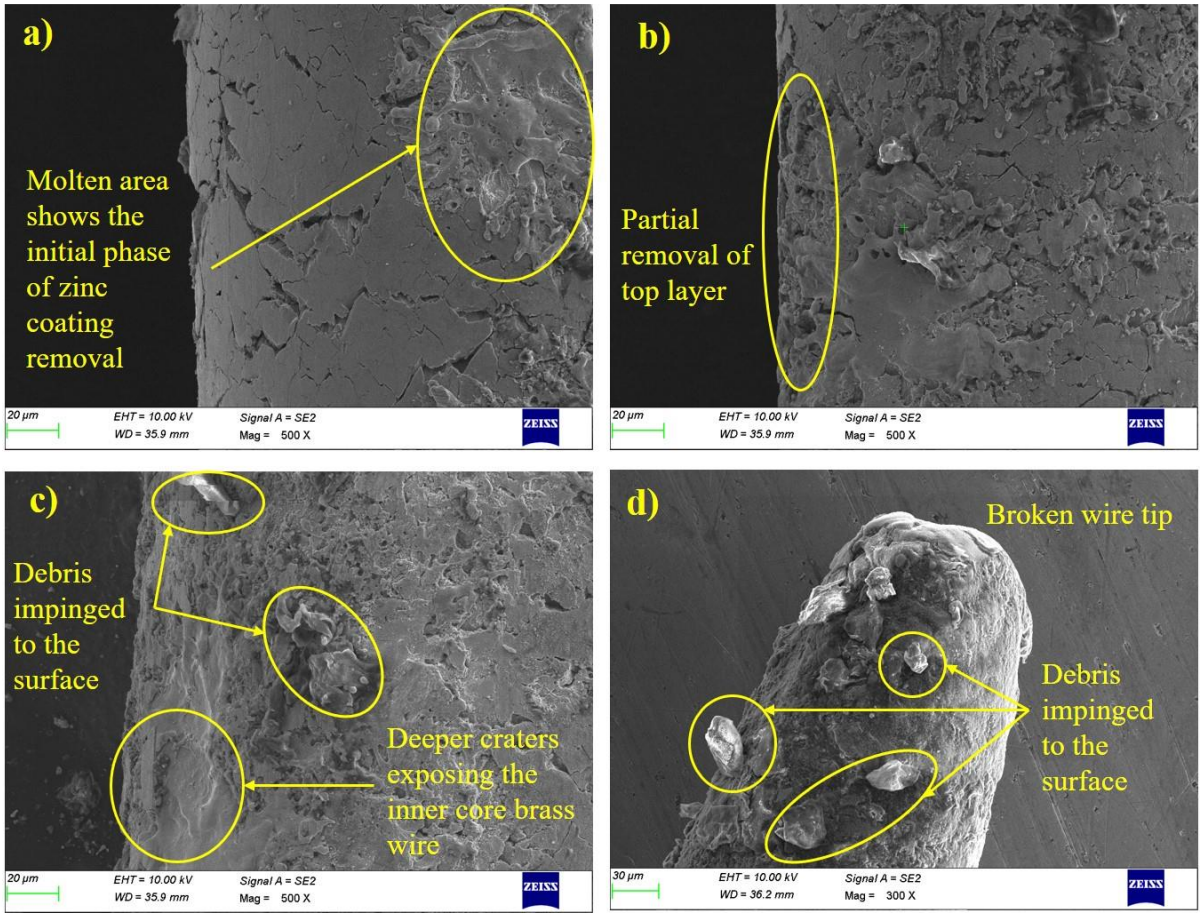

Fig. 8 Categories of wire wear (a) minimal degradation (Exp. No. 10) (b) intermediate degradation (Exp. No. 13) (c) severe degradation (Exp. No. 15) (d) failed wire tip (Exp. No. 6)

Once the inner core is exposed, as shown in Fig. 8 (c), any further wire wear by arc or short pulses will result in catastrophic wire breakages. This phenomenon is shown in Fig. 8 (d), which corresponds to experiment number 6. The wire breakages were caused by excessive debris accumulation, causing higher intensity sparks such as arcs and short circuits. If the relative proportion of these harmful sparks is greater, then the sparking frequency and discharge energy per spark will be higher. Owing to the short-circuit sparks, the exposed core brass wire develops deeper cracks and craters, which affect the wire strength. After a critical

point, the wire electrode can no longer withstand the load from the wire tension. At the point of most severe surface damage, the wire will start to elongate, reducing the wire diameter progressively and finally breaks it by a rupture at the point of minimum cross-section. Hence, the failed tip resembles a cone with significant wear on the surrounding and adjacent surfaces, as shown in Fig. 8 (d).

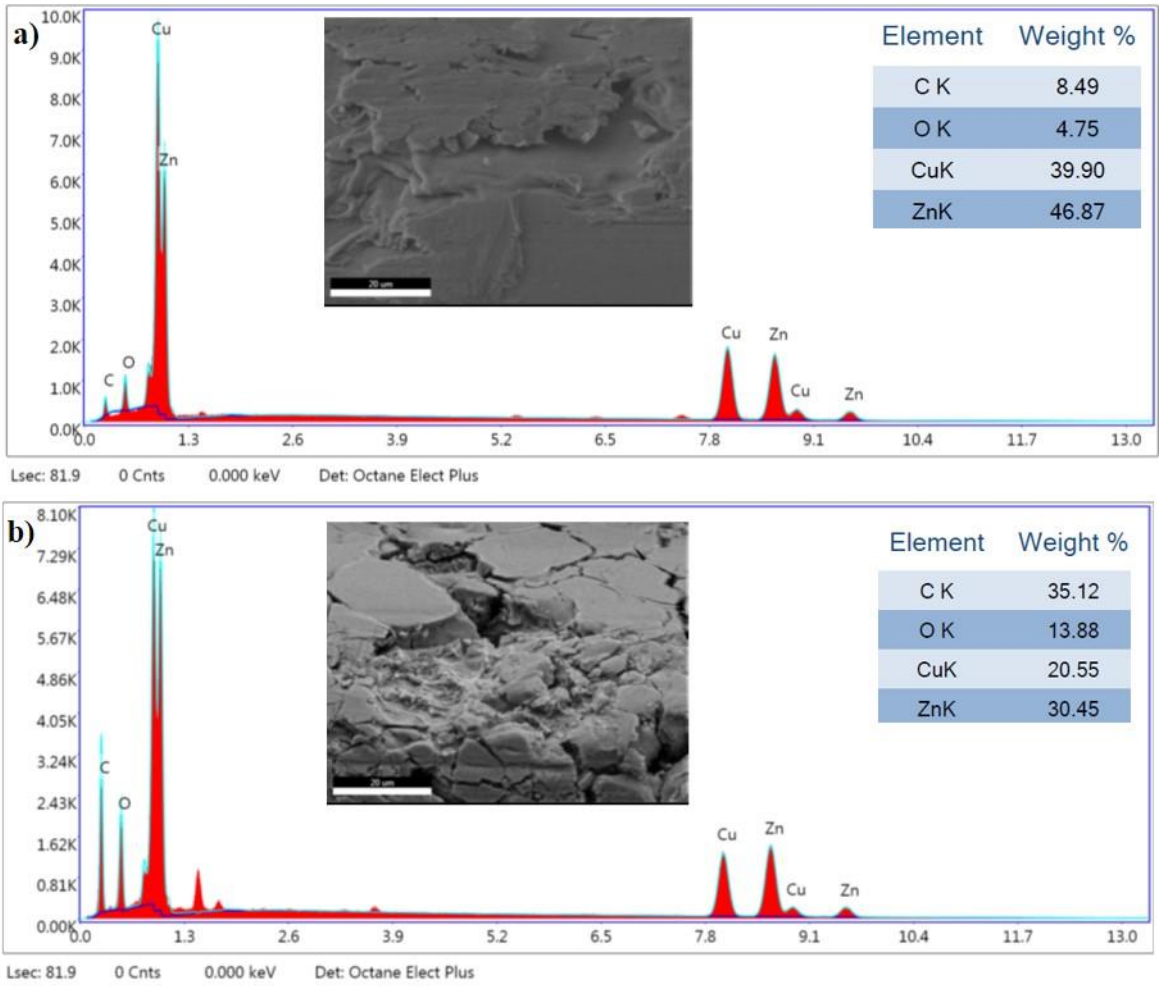

Fig. 9 EDS images of worn zinc coated brass wire surface at
(a) mild wire wear (Expt. No. 10) (b) severe wire wear (Expt. No. 15)

The energy-dispersive X-ray spectroscopy (EDS) analysis presented in Fig. 9 shows that the zinc weight percentage at the initial stages of wire wear (experiment number 10) was greater than that in the latter stages (experiment number 15). This confirms that one of the primary reasons for wire failures in coated wire electrodes is the excessive removal of wire coating due to higher intensity sparks. Furthermore, the carbon and oxygen contents were greater in the severe wear case, indicating more significant corrosive effects.

Table 8 Details of machining process failure situations

Type of failure	Exp no	Length machined (mm)	Time to failure (min)
Spark absence	7, 16, 17, 18, 19, 20, 22, 23, 24, 25, 26, 27	0	-
Wire breakage	28	4.61	3.12
	29	4.81	3.10
	30	4.64	3.09
	37	4.53	4.20
	38	3.91	3.86
	39	4.01	3.84
	40	4.57	3.16
	55	0.16	0.52
	56	0.32	0.61
	57	0.09	0.51
	58	0.44	0.72
	59	0.27	0.67
	60	0.33	0.68
	61	2.40	1.47
	64	2.37	1.38
	65	2.21	1.37
	66	2.36	1.37
	67	2.57	1.61
	68	2.02	1.60
	69	1.96	1.59

Table 8 shows the details of the process failures. In the case of 'spark absence failure', sparks were absent at the beginning of the cutting because of the gap, which did not allow the breakage of the dielectric barrier to produce sustained repetitive sparks. The earliest occurrence of wire breakage was observed at 0.09 mm. The final occurrence of wire breakage was observed at 4.81 mm. Failure occurred immediately after the commencement of machining for experiment numbers 55, 57, and 59. The pulse-on time was the highest at 120 μs; combining that with a minimum pulse of time of 20 μs and a lower spark gap setting of 20–40 V, sudden failure occurred. Because of high discharge energy, debris production was extremely high, and the time to remove the debris and the spark gap for efficient flushing was absent in those

conditions. This resulted in immediate debris accumulation and sudden failure within a minute. In a few other cases, machining continued for some distance before failure occurred (experiment numbers 28 to 30, and 37). This situation may not be as extreme as in the previous case, but it is still unfavorable for prolonged machining. Debris accumulation may have occurred gradually, which gradually resulted in spark gap bridging and finally wire rupture. The time for failure was calculated, and it was observed that all failures occurred within the first 5 min. Depending on the parameter settings, the total operating time for normal machining was 8–32 min.

3.3.2 Surface integrity variations during normal machining

The section compares the surface integrity of components machined by parameter settings classified as "normal machining."

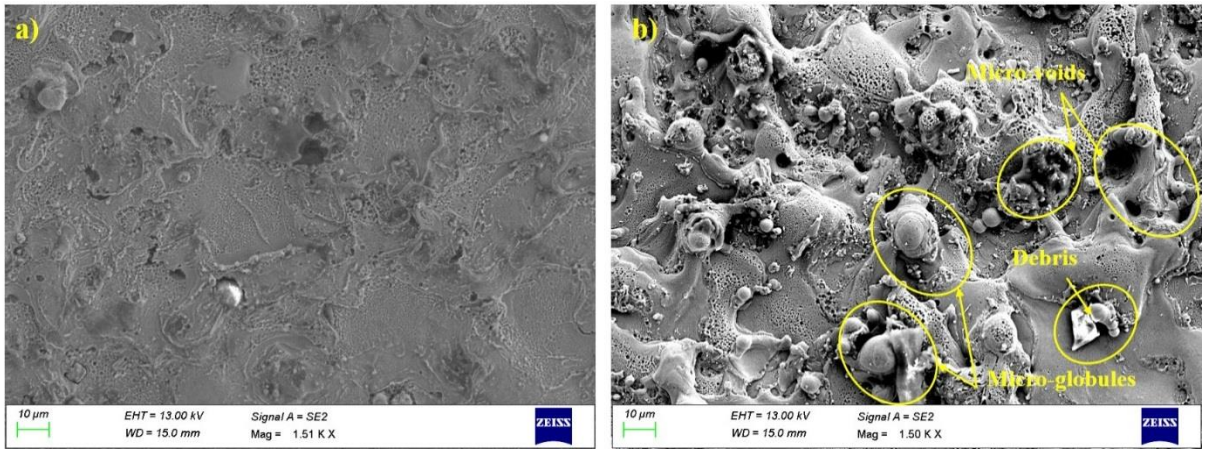

Fig. 10 FE-SEM images showing machined surface morphology after (a) Expt. No. 11 (b) Expt. No. 15

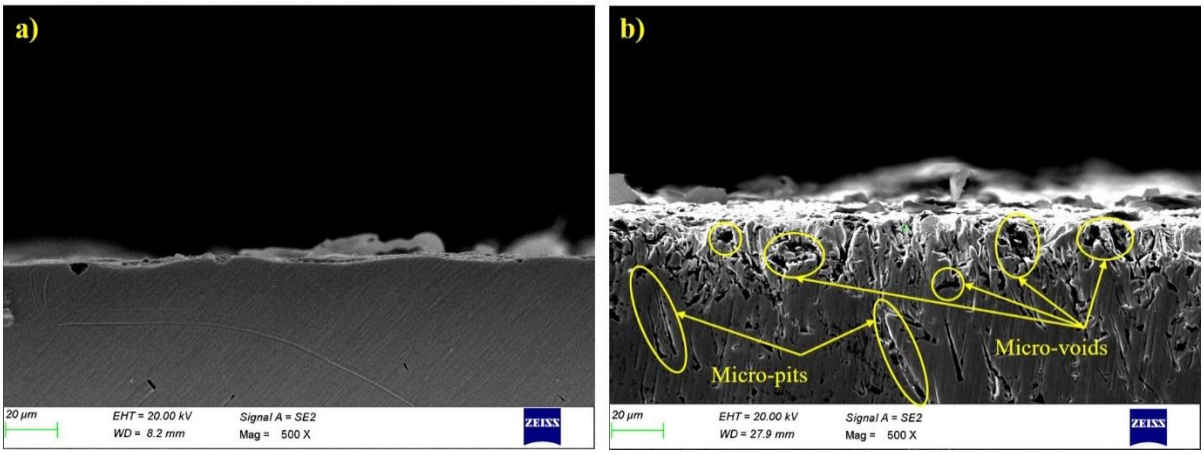

Fig. 11 Cross sectional view of machined surfaces under SEM after (a) Expt. No. 11 (b) Expt. No. 15

A surface morphology comparison for the normal machining scenario is shown in Figs. 10 and 11. Fig 10 (a) shows the SEM image of the machined surface corresponding to experiment number 11 of the confirmation experiments. Fig. 11 (a) shows a cross-sectional image of the same machined sample. Experiment 11 was conducted using the following parameters: a lower pulse-on time (T_{on}= 102 µs), higher pulse-off time (T_{off} = 51 µs), moderately high servo voltage (SV = 40 V), and moderately high wire feed rate (WF = 6 m/min). Consistent with the effects of the parameters discussed in the previous paragraph, a smooth surface with minimal surface defects was observed, as shown in Figs. 10 (a) and 11 (a). Fig. 10 (b) shows the SEM image of the machined surface corresponding to experiment number 15. Fig. 11 (b) shows the cross-sectional image of the machined surface of the same sample. In contrast to the previous case, the surface exhibited many microglobules, microvoids, and debris. Compared with the previous parameter combinations, experiment number 15 involved a higher pulse-on time (T_{on} = 117 µs), lower pulse-off time (T_{off} = 43 µs), and lower wire feed rate (WF = 4 m/min). The surface was coarser compared with that of the previous case owing to the combination of a higher discharge energy with poorer flushing conditions. Fig. 12 shows the surface morphology comparison of the machined surfaces for the cases above. A non-contact 3D profilometer was used to capture the images. Clearly, Fig. 12 (a) shows a smoother surface compared with Fig. 12 (b). Table 9 shows the surface roughness of the "normal" class from the confirmation tests. Consistent with the observations thus far, experiments 11 and 13 demonstrated the minimum and maximum roughness, respectively.

Table 9 Surface roughness comparison for 'Normal machining' in confirmation tests

S. No.	Input Parameters				R_a
	T_{on} (µs)	T_{off} (µs)	Servo voltage (V)	Wire feed (m/min)	
1	111	47	47	7	1.36
2	109	37	31	4	1.76
7	106	29	47	5	1.24
10	102	54	21	6	1.12
11	102	51	40	6	0.97
12	109	47	21	9	1.65
13	112	41	37	3	1.97
15	117	43	42	4	2.64
17	100	47	20	4	1.60
19	113	55	44	4	1.45

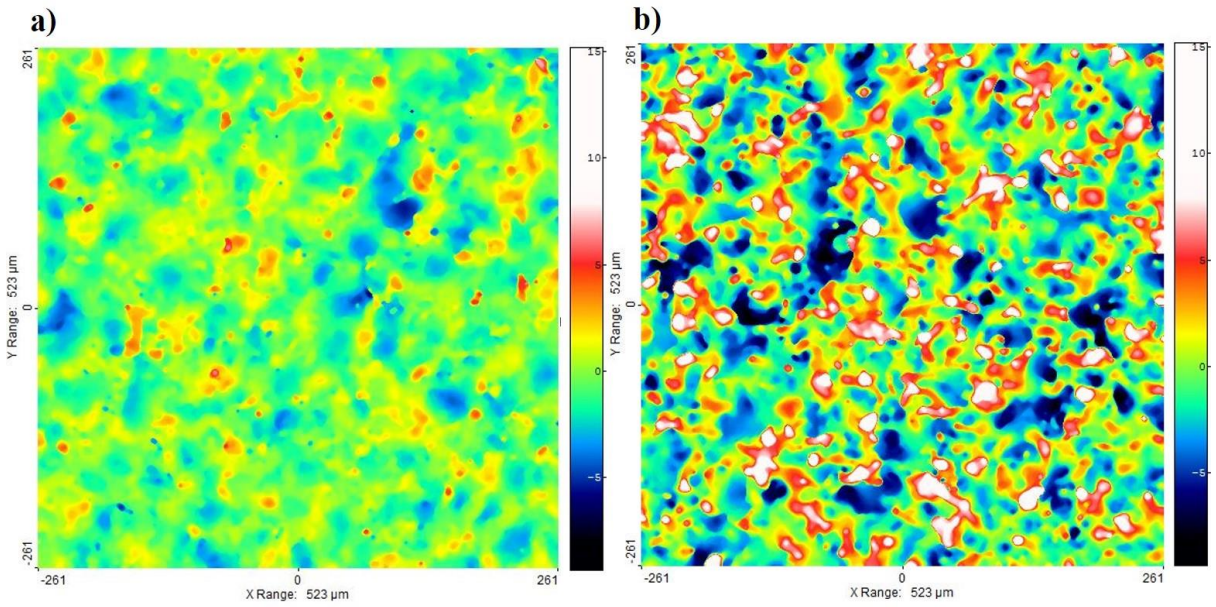

Fig. 12 Surface morphology comparison of machined surfaces using non-contact 3D profilometer images after (a) Expt. No. 11 (b) Expt. No. 15

Within the "normal machining" class, the surface integrity aspects (surface finish, morphology, recast layer thickness, elemental contamination, etc.) of the machined components can vary [30]. The acceptable level of surface finish or surface degradation (due to excessive cutting temperature) is application dependent. A separate optimization study considering the relevant responses is required to select an application-specific input parameter setting. Such an analysis was not attempted in this study but is planned for future studies.

5 Conclusions

A multiclass classification model was developed to classify the machining outcomes of wire-EDM Inconel 718. Because the parametric interactions were difficult to predict owing to the complex and stochastic nature of wire-EDMN, a classification model was necessitated to classify and predict the process failures. An ANN classification model, which is a computationally fast and easy option for failure prediction, was developed with an overall accuracy of 90%. Furthermore, confirmation tests were conducted to test the model performance in real-world machining situations. The model demonstrated a 95% prediction accuracy during the confirmation tests. The stages of wire wear leading to failure were analyzed for a coated wire electrode. Different microstructural images showed that zinc coating was removed by exposing the brass wire core, eventually resulting in failure by catastrophic wire

rupture. The parametric dependence of the machined surface quality was discussed by comparing SEM images obtained.

Acknowledgements

The authors would like to acknowledge the Central Instrumentation Facility (CIF), Indian Institute of Technology Palakkad for their support in this work.

References

1. Ho KH, Newman ST, Rahimifard S, Allen RD (2004) State of the art in wire electrical discharge machining (WEDM). Int J Mach Tools Manuf 44:1247–1259. https://doi.org/10.1016/j.ijmachtools.2004.04.017
2. Mandal A, Dixit AR (2014) State of art in wire electrical discharge machining process and performance. Int J Mach Manu Mater 16:1. https://doi.org/10.1504/IJMMM.2014.063918
3. Saha S, Pachon M, Ghoshal A, Schulz MJ (2004) Finite element modeling and optimization to prevent wire breakage in electro-discharge machining. Mech Res Commun 31:451–463. https://doi.org/10.1016/j.mechrescom.2003.09.006
4. Fedorov AA, Blesman AI, Postnikov D V., et al (2018) Investigation of the impact of Rehbinder effect, electrical erosion and wire tension on wire breakages during WEDM. J Mater Process Technol 256:131–144. https://doi.org/10.1016/j.jmatprotec.2018.02.002
5. Gamage JR, Desilva AKM (2016) Effect of Wire Breakage on the Process Energy Utilisation of EDM. Procedia CIRP 42:586–590. https://doi.org/10.1016/j.procir.2016.02.264
6. Okada A, Konishi T, Okamoto Y, Kurihara H (2015) Wire breakage and deflection caused by nozzle jet flushing in wire EDM. CIRP Ann - Manuf Technol 64:233–236. https://doi.org/10.1016/j.cirp.2015.04.034
7. Yeo SH, Ngoi BKA, Poh LS, Hang C (1997) Cost-tolerance relationships for non-traditional machining processes. Int J Adv Manuf Technol 13:35–41. https://doi.org/10.1007/BF01179228
8. D'Urso G, Quarto M, Ravasio C (2017) A model to predict manufacturing cost for micro-EDM drilling. Int J Adv Manuf Technol 91:2843–2853. https://doi.org/10.1007/s00170-016-9950-0

9. D'Urso G, Giardini C, Quarto M, Maccarini G (2017) Cost index model for the process performance optimization of micro-EDM drilling on tungsten carbide. Micromachines 8:. https://doi.org/10.3390/mi8080251
10. Gisario A, Mehrpouya M, Rahimzadeh A, et al (2020) Prediction model for determining the optimum operational parameters in laser forming of fiber-reinforced composites. Adv Manuf 8:242–251. https://doi.org/10.1007/s40436-020-00304-3
11. Zhao QJ, Huang CH, Ke ZN, Yi JG (2017) Recognition results classification and post-processing methods for painted characters on billet surface. Adv Manuf 5:261–270. https://doi.org/10.1007/s40436-017-0190-9
12. Markopoulos AP, Manolakos DE, Vaxevanidis NM (2008) Artificial neural network models for the prediction of surface roughness in electrical discharge machining. J Intell Manuf 19:283–292. https://doi.org/10.1007/s10845-008-0081-9
13. Ong P, Chong CH, bin Rahim MZ, et al (2020) Intelligent approach for process modelling and optimization on electrical discharge machining of polycrystalline diamond. J Intell Manuf 31:227–247. https://doi.org/10.1007/s10845-018-1443-6
14. Maity K, Mishra H (2018) ANN modelling and Elitist teaching learning approach for multi-objective optimization of μ -EDM. J Intell Manuf 29:1599–1616. https://doi.org/10.1007/s10845-016-1193-2
15. Liao YS, Chu YY, Yan MT (1997) Study of wire breaking process and monitoring of WEDM. Int J Mach Tools Manuf 37:555–567. https://doi.org/10.1016/S0890-6955(95)00049-6
16. K. P. Rajurkar; W. M. Wang (1991) On-Line Monitor and Control for Wire Breakage in WEDM. Ann CIRP 40:219–222. https://doi.org/10.1016/j.procir.2017.12.059
17. Yan MT, Liao YS (1996) A self-learning Fuzzy controller for wire rupture prevention in WEDM. Int J Adv Manuf Technol 11:267–275. https://doi.org/10.1007/BF01351284
18. Wang WM, Rajurkar KP (1992) Monitoring sparking frequency and predicting wire breakage in WEDM. In Winter Annual Meeting of the American Society of Mechanical Engineers. Publ by ASME. 49-64.
19. Luo YF (1999) Rupture failure and mechanical strength of the electrode wire used in wire EDM. J Mater Process Technol 94:208–215. https://doi.org/10.1016/S0924-0136(99)00107-7
20. Kwon S, Yang MY (2006) The benefits of using instantaneous energy to monitor the transient state of the wire EDM process. Int J Adv Manuf Technol 27:930–938. https://doi.org/10.1007/s00170-004-2252-y

21. Cabanes I, Portillo E, Marcos M, Sánchez JA (2008) An industrial application for on-line detection of instability and wire breakage in wire EDM. J Mater Process Technol 195:101–109. https://doi.org/10.1016/j.jmatprotec.2007.04.125
22. Liao YS, Woo JC (2000) Design of a fuzzy controller for the adaptive control of WEDM process. Int J Mach Tools Manuf 40:2293–2307. https://doi.org/10.1016/S0890-6955(00)00036-5
23. Bufardi A, Akten O, Arif M, Xirouchakis P (2017) Towards zero-defect manufacturing with a combined online - offline fuzzy-nets approach in wire electrical discharge machining. WSEAS Transactions on Environment and Development, 13. pp. 401-409.
24. Kumar R, Choudhury SK (2011) Prevention of wire breakage in wire EDM. Int J Mach Mach Mater 9:86–102. https://doi.org/10.1504/IJMMM.2011.038162
25. Mukherjee I, Ray PK (2006) A review of optimization techniques in metal cutting processes. Comput Ind Eng 50:15–34. https://doi.org/10.1016/j.cie.2005.10.001
26. Caggiano A, Teti R, Perez R, Xirouchakis P (2015) Wire EDM monitoring for zero-defect manufacturing based on advanced sensor signal processing. Procedia CIRP 33:315–320. https://doi.org/10.1016/j.procir.2015.06.065
27. Samanta B, Al-Balushi KR, Al-Araimi SA (2006) Artificial neural networks and genetic algorithm for bearing fault detection. Soft Comput 10:264–271. https://doi.org/10.1007/s00500-005-0481-0
28. Wang ZY, Rajurkar KP, Fan J, et al (2003) Hybrid machining of Inconel 718. Int J Mach Tools Manuf 43:1391–1396. https://doi.org/10.1016/S0890-6955(03)00134-2
29. Prohaszka J, Mamalis AG, Vaxevanidis NM (1997) The effect of electrode material on machinability in wire electro-discharge machining. J Mater Process Technol 69:233–237. https://doi.org/10.1016/S0924-0136(97)00024-1
30. Abhilash PM, Chakradhar D (2020) Surface integrity comparison of wire electric discharge machined Inconel 718 surfaces at different machining stabilities. Procedia CIRP 87:228–233. https://doi.org/10.1016/j.procir.2020.02.037